metals

MDPI

Article

The Influence of Austenite Grain Size on the Mechanical Properties of Low-Alloy Steel with Boron

Beata Białobrzeska *, Łukasz Konat and Robert Jasiński

Department of Materials Science, Welding and Strength of Materials, Wrocław University of Technology, 50-370 Wrocław, Poland; lukasz.konat@pwr.edu.pl (Ł.K.); robert.jasinski@pwr.edu.pl (R.J.)
* Correspondence: beata.bialobrzeska@pwr.edu.pl; Tel.: +48-713203845

Academic Editor: Robert Tuttle
Received: 21 November 2016; Accepted: 12 January 2017; Published: 17 January 2017

Abstract: This study forms part of the current research on modern steel groups with higher resistance to abrasive wear. In order to reduce the intensity of wear processes, and also to minimize their impact, the immediate priority seems to be a search for a correlation between the chemical composition and structure of these materials and their properties. In this paper, the correlation between prior austenite grain size, martensite packets and the mechanical properties were researched. The growth of austenite grains is an important factor in the analysis of the microstructure, as the grain size has an effect on the kinetics of phase transformation. The microstructure, however, is closely related to the mechanical properties of the material such as yield strength, tensile strength, elongation and impact strength, as well as morphology of occurred fracture. During the study, the mechanical properties were tested and a tendency to brittle fracture was analysed. The studies show big differences of the analysed parameters depending on the applied heat treatment, which should provide guidance to users to specific applications of this type of steel.

Keywords: boron steels; austenite grain size; impact strength; fracture; tensile strength

1. Introduction

The grain size has a measurable effect on most of the mechanical properties. For example, at room temperature, the hardness, yield strength, tensile strength, fatigue strength, and impact strength all increase with decreasing grain size. The influence of grain size on the mechanical properties of steel is most commonly expressed in a Hall-Petch Equation (Equations (1) and (2)) [1–4]. This classic equation can also be used to predict hardness. A similar equation applies to the brittle cracking (cleavage fracture stress, σ_f) of high-strength steels (Equation (3)). According to this criterion, increase in the grain size eases the cracking process, because the greater the number of dislocations that pile up, the less stress is required for crack development [5].

$$\sigma_y = \sigma_0 + \frac{k_y}{\sqrt{d}} \quad (1)$$

where:

σ_y yield stress;
σ_0 the friction resistance for dislocation movement within the polycrystalline grains;
k_y a measure of the local stress needed at a grain boundary for the transmission of plastic flow—unpinning constant;
d the average grain size.

The value of the k_y coefficient in Equation (1) has been described with the following relationship:

$$k_y \approx 3\left[\frac{2Gb\tau_b}{q\pi}\right]^{1/2} \tag{2}$$

where:

G modulus of rigidity (shear);
b Burgers vector (dependent on the type of crystal lattice);
q geometrical factor (dependent on the type of crystal lattice);
τ_b critical stress required for passing the slide through the grain boundary [2].

$$\sigma_f = \sigma_{0f}\frac{k_f}{\sqrt{d}} \tag{3}$$

where:

σ_f fracture stress;
σ_{0f} and k_f the experimentally determined constants, and $k_f > k_y$ from Equation (2) has the following value:

$$k_f \geq \left(\frac{6\pi\gamma G}{1-\nu}\right)^2 \tag{4}$$

where:

γ surface energy of a crack;
ν Poisson's ratio.

However, Morris [4] noticed that the Hall-Petch equation is not unequivocal for martensitic steels. Some studies concerning the influence of the prior austenite grain size on the austenite to ferrite transformation temperature and different ferrite morphologies in Nb-micro-alloyed (HSLA) steel have been performed [6]. Similar studies have been performed to investigate the impact of the prior austenite grain size on the morphology and mechanical properties of martensite in medium carbon steel [3] and to predict the austenite grain growth in low-alloy steels [7], but there is still a lack of knowledge about the influence of the prior austenite grain size on the basic mechanical properties in low-alloy boron steels with high resistance to abrasive wear.

In recent times, in various industries, increasingly frequent attempts have been made to increase the durability of machine elements by applying boron to the construction of a low-alloy, high-strength steel. This group of materials includes, among others, constant Hardox. By using the advanced technology of their production, these steels achieve high abrasive wear resistance in combination with high strength and a sufficient toughness. Due to the fact that the technologies used in industrial conditions require the structural materials to be tolerant of complex thermal or thermal-plastic processes, an important factor determining the properties of these materials is the austenite grain size. So far, the knowledge of these advanced steels is not sufficient, and publicly available information about them is mere advertising. Therefore, an analysis of the growth of austenite grains in these steels according to the austenitizing temperature in order to prevent the degradation of their very favorable mechanical properties appears to be justified. These steels are exposed to the degradation of their favorable properties due to the thermal processes used for assembling components made of these steels. Therefore, it is important to control the grain size of these steels during their thermal treatment. This study analyzed the growth of austenite grains in, for example, Hardox 450, which is widely used in industry.

Another very important issue, from the point of view of the impact resistance level achieved in the low-alloy steels, is related to the type and morphology of the martensite structure. As a result of

transformation in the low- and medium-carbon steels, martensite initially nucleates in random areas of austenite grain, and its growth takes place afterward [8]. A martensite area created in this way, after reaching the grain boundary, may initiate further development of martensitic areas in neighbouring grains, according to the analogous variant. The whole process is autocatalytic in character. It results from the way of passing stress (through the grain boundaries) caused by the greater specific volume of martensite in relation to austenite. Accordingly, it can be stated that the greater degree of heterogeneity of crystallographic orientation variants of the formed martensite corresponds to a larger number of initial nuclei [8–10]. A characteristic feature of martensite created in this way is the three-level hierarchy of morphology, consisting of laths, blocks, and packets. The laths of martensite, creating a block, have the same crystallographic orientation and thus represent the same variant of the martensite structure formed. By contrast, the packets are created by clusters of blocks of the same habitus plane, corresponding to the plane $\{111\}\gamma$ of the primary austenite. In the simplified version of considerations (neglecting the chance of separate blocks of martensite of the same variant appearing in one austenite grain), it can be stated that, in the single packet blocks of martensite, a maximum of six variants may be present. This results from six possible crystallographic directions within one plane {111} of austenite, of which austenite has four. In relation to that, in a single grain of prior austenite, 24 different variants of martensite may appear simultaneously at the wide-angle inter-block boundaries [1,11].

From the point of view of the static strength and the impact resistance of the low- and medium-carbon steel, their direct dependence on the size of blocks and packets, which constitute the effective dimensions of the martensitic structure in the meaning of the Hall-Petch relationship, has to be underlined. From the data contained in the works [1–3], decrease in the grain size of the primary austenite (and thus the reduction of the martensite packets sizes) from 200 µm to 5 µm results in an increase in strength of 235 MPa and an eight-fold increase in steel impact resistance. In relation to the above, in the opinion of the authors of this work, it is worth analyzing the morphology and size of the packets of martensitic structure while considering the impact of the grain size of the prior austenite on the selected mechanical properties of low-alloy steels with boron.

2. Materials and Methods

For the tests, Hardox 450, a material from a group of low-alloy boron steels with a high resistance to abrasive wear, was selected [12–15]. All samples were taken from the longitudinal direction relative to the sheet rolling direction. The chemical composition and mechanical properties of the analyzed material (according to the manufacturer's data and the research data) are presented in Tables 1 and 2. The plate thickness was 30 mm. Chemical composition analysis was performed with a spectral method using a glow-discharge spectrometer. The content of oxygen and nitride was measured using a NO determinator.

Table 1. Selected mechanical properties of the investigated steel in the as-received condition. KCV: notched impact strength.

Mechanical Properties	$R_{p0.2}$ (MPa)	Hardness (HB)	KCV_{-20} (J/cm^2)
Manufacturer's data [12]	1100–1300	425–75	27

Table 2. Chemical composition of the investigated steel.

Element (wt %)	C	Mn	Si	P	S	Ni	Cr	V	Al	Ti
Content of elements	0.223	1.32	0.489	0.009	0.004	0.044	0.784	0.004	0.035	0.02
Element (wt %)	**Nb**	**B**	**Cu**	**Co**	**Mo**	**As**	**Pb**	**O**	**N**	
Content of elements	0.005	0.0011	0.015	0.016	0.012	0.009	0.002	0.049885	0.003805	

The metallographic studies were performed using a light microscope (Nikon Corporation, Tokyo, Japan). The microstructure in the as-received condition of the investigated steel is presented in

Figure 1. The tested material in the as-received state showed a structure of low-carbon martensite. The martensitic microstructure exhibits a high homogeneity and some features that can be described as being similar to tempered martensite, with precipitates of some non-metallic inclusions like titanium nitrides.

Figure 1. The microstructure of the investigated low-alloy boron steel with a high resistance to abrasive wear in the as-received state. Etched state, light microscope.

Samples were austenitized for a holding time of 20 min at temperatures of 900, 1000, 1100, and 1200 °C and then quenched in water. After each heat treatment, the samples of the prior austenite grain were tempered at 250 °C for 30 min, in order to retain the detail of the austenite microstructure and to allow identification of the prior austenite grain boundaries. The samples were etched with 5% picric acid at a temperature of 55 °C in accordance with the standard PN-H-04503:1961P. The measurements of the austenite grain size were performed using the program NIS Elements. Each average austenite grain size was evaluated from 100 measurements.

Packet size was measured using the linear intercept method on SEM images. About 100 martensite packets in each sample were measured to obtain the average packet size.

In order to determine the impact of heat treatment on the basic mechanical and plastic properties of the tested steel, tensile testing was conducted at ambient temperature, based on the valid standard PN-EN ISO 6892-1:2010 (metallic materials—tensile testing). The research was carried out on an Instron 5982 machine (Instron, High Wycombe, UK) using an extensometer to measure elongation. Proportional rectangular samples were tested with an original gauge length of L_0 = 35 mm. Testing rates were based on stress rate (Method B according to the ISO Standard 6892). Within the elastic and plastic range up to the yield strength, the strain rate was 0.002 1/s; after the yield strength, the stress rate exceeded 25 MPa/s until fracture occurred. The following mechanical properties were determined: non-proportional extension (yield strength, $R_{p0.2}$), tensile strength (R_m), percentage elongation after fracture (A), and percentage reduction of area (Z).

In order to determine the value of the absorbed energy (KV), the notched impact strength (KCV), and the type of fracture related to the austenitic temperature, a Charpy impact test was performed. The study was performed in accordance with Standard PN-EN ISO 148-1:2010 (Metallic materials—Charpy pendulum impact test) on the Zwick Roell pendulum hammer RPK300 (Zwick Roell Gruppe, Ulm, Germany) using an initial energy of 300 J. Standard samples, V-notched to a depth of 2 mm, were tested. The tests were carried out after the samples were cooled to -40 ± 2 °C and conditioned for 15 min in a mixture of liquid nitrogen and isopropanol. The temperature was monitored using a digital thermometer Center (Center Technology Corp., New Taipei City, Taiwan), and the transfer time for all samples was less than 5 s. Fractographic analysis was performed using a stereo microscope (Nikon Corporation, Tokyo, Japan) and SEM (JEOL Ltd., Tokyo, Japan).

Samples for mechanical research were cut in the longitudinal direction to the rolling direction.

3. Results

3.1. Austenite Grain Growth Analysis

A comparison of the austenite grain size attained after changing the temperature from 900, 1000, 1100, and 1200 °C for 20 min is presented in Figures 2 and 3.

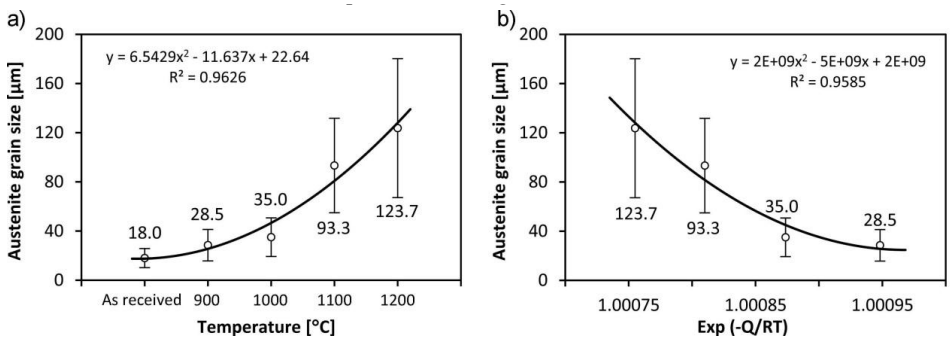

Figure 2. Austenite grain size (**a**) in the as-received state and at different austenitizing temperatures; (**b**) as an Arrhenius plot.

The austenite grain growth with increasing austenitizing temperature was approximated with a quadratic function at the level of correlation $R^2 = 0.96$. An approximation of the results with this model is consistent with the model shown in [8].

The measurement results of austenite grain size in the as-received state are shown in Figure 3a. The sample in the as-received state is characterized by the lowest grain size. The values vary within the range 6–38 µm. The average value is approximately 18.0 ± 7.8 µm. The manufacturer did not provide details of heat treatment in addition to information about hardening and tempering [12]. The distribution was approximated with a logarithmic normal model. This model is similar to the distribution of austenite grains size presented in [16]. Almost 50% of the measurements are grains with a diameter of 10–20 µm. Abnormal grains were not observed (Figure 4a).

The austenitizing process at a temperature of 900 °C caused an increase in the average grain size by nearly 60%, compared to the as-received state. The size varies between 12 and 58 µm. The average value is 28.5 ± 12.8 µm. Again, abnormal grains were not observed (Figure 4b). The measurement results are approximated with a logarithmic function. The most common diameters of grains were across the ranges 11–18 µm and 32–39 µm (Figure 3b).

During the austenitizing at 1000 °C, the minimum measured grain size was approximately 13.5 µm. This value is more than 2 times higher than that measured in the as-received state (i.e., 6 µm). The average grain size is 35.0 ± 15.7 µm. Grains from 10 to 19 µm constitute 24% (Figure 3c). However, a higher frequency of grains in the range of approximately 60–70 µm is found (Figure 3c). The frequency of occurrence of each austenite grain size cannot be approximated with any mathematical model.

Austenitizing at 1100 °C caused the appearance of clearly abnormal austenite grains. Their maximum size ranged from 211 to 296 µm (Figure 4d). They were not included in the calculation of the average grain size. Grain sizes in the ranges of 50–69 µm and 107–126 µm occurred more frequently than others (Figure 3d). The average size of the austenite grains is 93.3 ± 38.4 µm.

The structure obtained after austenitizing at 1200 °C is significantly different from the others (Figure 4e). There is a strong grain growth, and the fine-grained regions disappear. The average grain size is 123.7 ± 56.5 µm. This is about three times higher than that obtained at 900 °C. Comparing the results obtained for the sample in as-received state, there was a five-fold growth of the average austenite grain size. Seventy-one percent of the grain diameters are of a value exceeding 100 µm, of

which 13% are grains with a diameter greater than 200 µm. The results are presented in graphical form and approximated with a logarithmic model (Figure 3e).

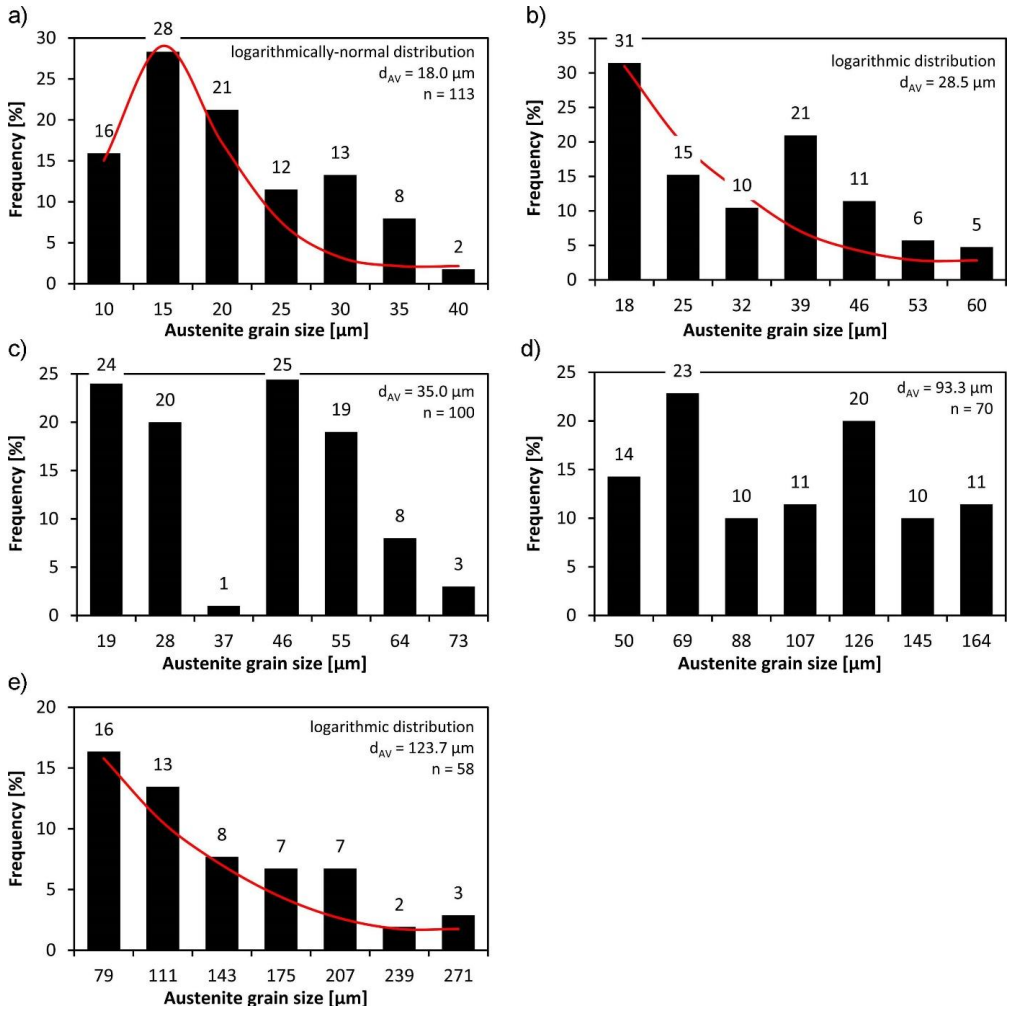

Figure 3. The frequency of occurrence of austenite grain size of the tested steel: (**a**) in the as-received state; (**b**) after austenitizing at 900 °C, 20 min; (**c**) after austenitizing at 1000 °C, 20 min; (**d**) after austenitizing at 1100 °C, 20 min; (**e**) 1200 °C, 20 min.

The migration of grain boundaries can be compared to a diffusion process. Therefore, the grain growth rate increases with an increase in the holding temperature. It can be seen in Figure 4b that the growth of austenite grains is gradual at a low austenitizing temperature. The abnormal grains are presented in the microstructure after heating at 1000 °C (Figure 4c), 1100 °C (Figure 4d), and 1200 °C (Figure 4e). The difference between these microstructures is in the number of fine grains. The decrease in the number of fine grains indicates that larger austenite grains can merge from smaller ones and grow gradually with the increase in holding temperature. The abnormal grains develop in areas where fine grains are embedded. These fine grains surround the abnormal grains. When the fine grain areas disappear, the normal growth of the coarse grains can take place.

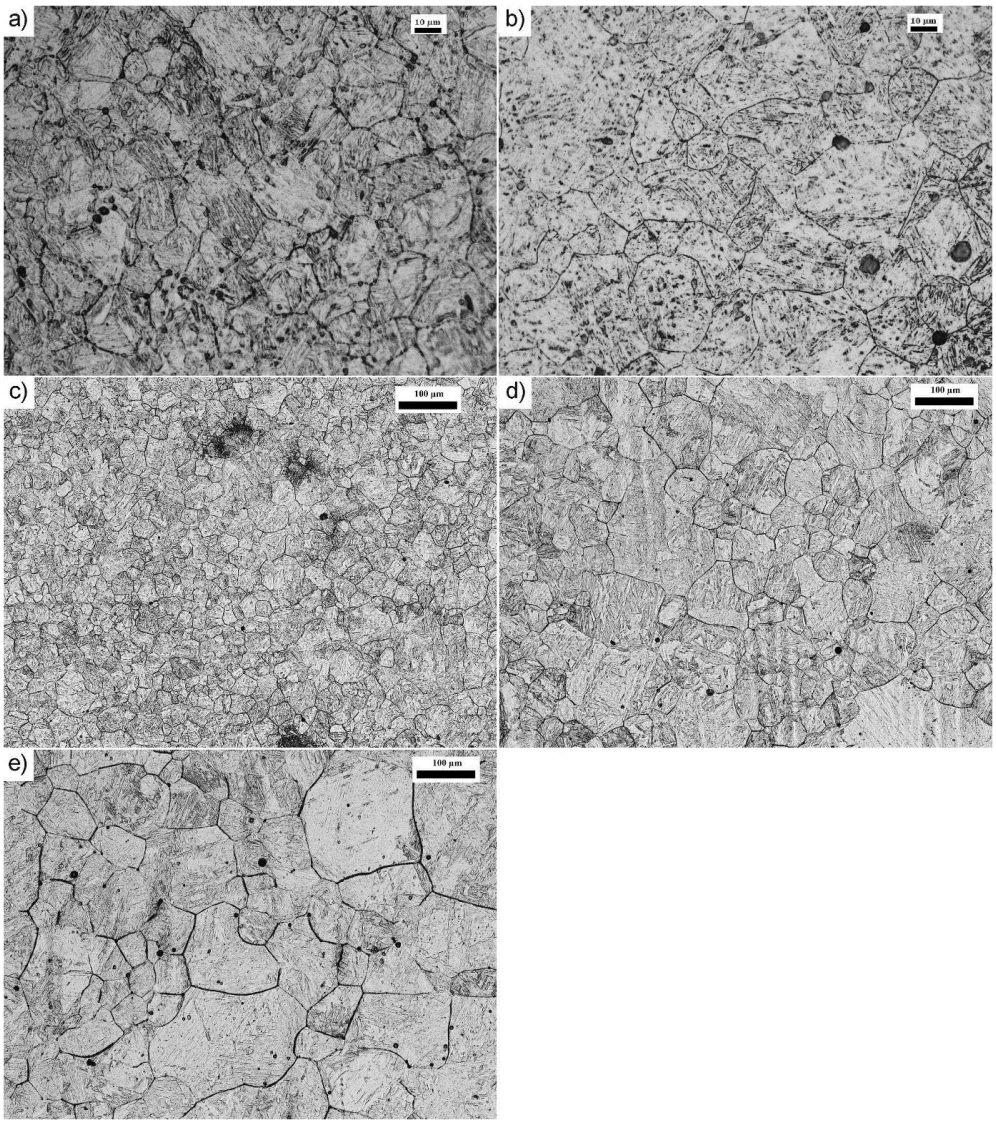

Figure 4. Micrographs of austenite grain boundaries in the as-received state and under different annealing conditions: (**a**) in the as-received state; (**b**) 900 °C, 20 min; (**c**) 1000 °C, 20 min; (**d**) 1100 °C, 20 min; (**e**) 1200 °C, 20 min. Etched state, light microscope.

3.2. The Tensile Test and the Impact Strength Test

The values of the mechanical properties determined during the tensile tests and impact strength test are presented in Table 3.

Table 3. Selected mechanical properties of tested steel after austenitizing at different temperature.

Austenitizing Temperature T (°C)	Tensile Strength R_m (MPa)	Yield Strength $R_{p0.2}$ (MPa)	Elongation A (%)	Reduction of Area Z (%)	Impact Strength KCV_{-40} (J/cm^2)
As received state	1433	1106	14.6	46	70
900	1445	1076	14.1	41	49
1000	1413	1016	13.2	37	38
1100	1425	1006	12.9	37	30
1200	1382	987	12.6	39	19

The results of the tensile tests show a decrease in percentage elongation after fracture (A) associated with increasing the austenitizing temperature from 900 to 1200 °C (Figure 5a). The relative

change of its value between the austenitizing temperatures of 900 and 1000 °C is more than 6%, between the austenitization temperatures of 1000 and 1100 °C, 2%, and between the austenitization temperatures of 1100 and 1200 °C, also about 2%. The total relative change of percentage elongation between the temperatures of 900 and 1200 °C is about 11%. As can be seen, the greatest decrease in percentage elongation took place after austenitizing at 1000 °C, when the austenite grains growth was about 22%. However, a further rise in austenitizing temperature does not cause rapid degradation of the ductile values represented by percentage elongation, despite the appearance of abnormal grains and a sharp increase in the austenite grain size between the austenitization temperatures of 1100 and 1200 °C. After austenitization at 1200 °C, the austenite grain is the greatest, followed by a decrease in the percentage elongation values, but its value is still maintained at a satisfactory level.

In the case of the percentage reduction of area (Z), the situation is similar (Figure 5b). There has been a decline in the value of the reduction of area of about 5%. Worth particular mention is the fact that there is no difference between the percentage reduction of area after austenitization at 1000 and 1100 °C, although the relative increase in austenite grain size connected with the appearance of abnormal grains was then considerable and amounted to 166.6%.

The highest values of plastic properties (A = 15%; Z = 47%) were noted for the as-received state characterized with the finest grains of austenite.

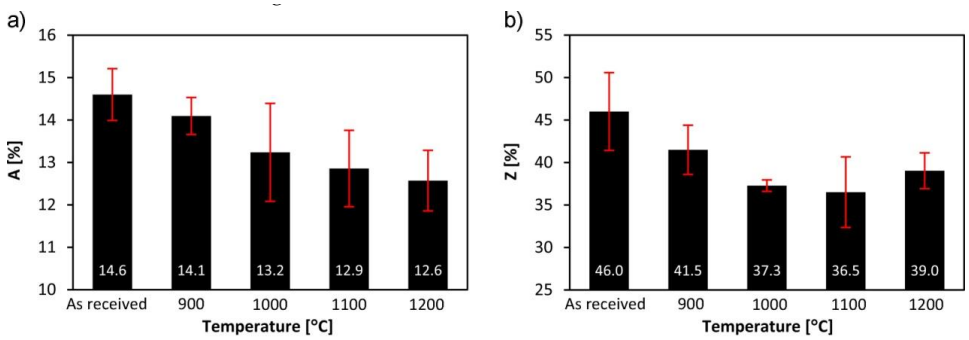

Figure 5. Percentage elongation (**a**) and percentage reduction of area (**b**) of the tested steel in the as-received state and after different austenitization temperatures.

The characteristic downward trend can also be noticed in the case of the values of the yield strength ($R_{p0.2}$) (Figure 6a) and the tensile strength (R_m) (Figure 6b), and is associated with an increase in austenitization temperature. It is worth noticing that, after austenitization at 900 °C, the tensile strength value is higher than in the as-received state, but the yield strength value is lower.

However, the continued downward trend in the case of tensile strength is not strong. Note that, after austenitizing at 1100 °C, the tensile strength was higher than the austenitizing at a lower temperature. The highest decrease in tensile strength of about 3% was noted between the austenitizing temperatures of 1100 and 1200 °C. The total decline in the value of tensile strength within the extreme range of austenitization temperatures was more than 4%.

A greater decrease was noticed in the case of the yield strength, even from the austenitization temperature of 1000 °C. The yield strength after austenitizing at this temperature decreased by about 6% in comparison to the yield strength after austenitizing at 900 °C. At higher temperature, the decrease in the yield strength value was not as significant and was about 1% and 2%, respectively, between samples austenitized at 1000 and 1100 °C and between samples austenitized at 1100 and 1200 °C. The overall decrease in yield strength within the extreme austenitization temperature range was more than 8% and two times higher than the decrease in the value of tensile strength.

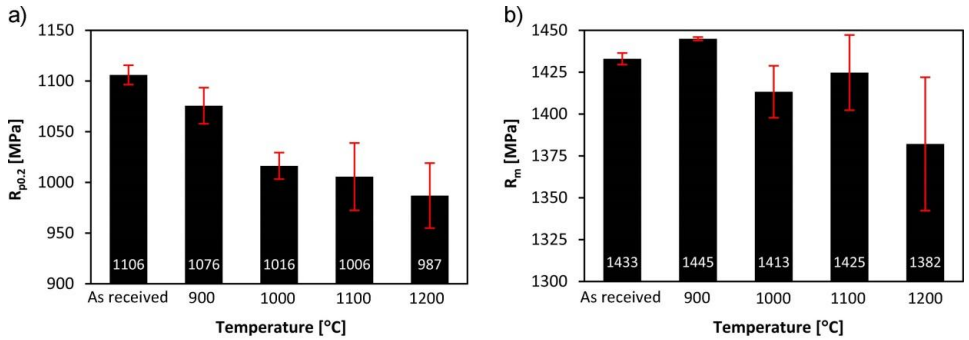

Figure 6. Tensile strength (**a**) and yield strength (**b**) of tested steel in the as-received state and after different austenitizing temperatures.

The tested material after austenitizing at different temperatures is characterized by the different resistance to brittle fracture, which in many applications has fundamental importance. Comparing the obtained values of impact strength, it is found that the impact strength decreases by nearly 61% between the average values for extreme austenitizing temperatures, confirming the trend determined in the tensile testing and unambiguously attesting to a drop in the plastic properties of the material (Figure 7). However, it can be seen that the impact of the austenitic temperature was stronger in the case of impact strength. Of interest is the very high impact strength value in the as-received state, which is characterized by the smallest austenite grain size. The difference in austenite grain size between the as-received state and the state after austenitizing at 900 °C is about 58%; however, the impact strength value drops by about 30%. This proves that the impact strength is very sensitive to the austenite grain size.

Assuming the criterion of a minimum impact strength equal to 35 J/cm^2, this steel meets this criterion until the austenitization temperature reaches 1000 °C. After austenitizing at a temperature of 1100 °C, the impact strength of this steel was 30 J/cm^2, which was not much lower than the criterion cited. The criterion of a minimum impact strength equal to 35 J/cm^2 is adopted for construction materials in many applications [17].

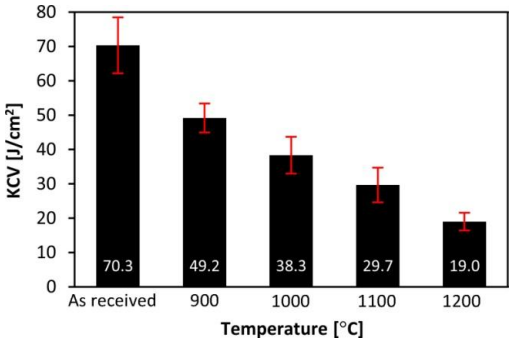

Figure 7. Impact strength KCV of tested steel in the as-received state and after different austenitizing temperatures.

3.3. Analysis of Martensite Morphology

Figure 8 presents the morphology of the martensitic structure of Hardox 450 steel in different states of heat treatment. In all the analyzed cases, the created martensite was in the form of laths laid in packets inside the prior austenite grains. The dependence between the size of the martensite packets and the size of the former austenite is shown in Figure 9. It has been shown that the size of the packets increased as a function of the heat treatment state of the steel (growth of the austenite grain). The average size of the packets increased from 3 µm to 16 µm, which corresponds to the

former austenite grain growth within the range of 18–124 μm. The increase in the packet size growth represents approximately the linear function. Figure 10 illustrates the distribution of the corresponding fractions of the martensite packets for the samples of different sizes of grain of the former austenite. At the base of the performed normal distributions, there is a high correlation of the appearance of the martensite fraction with the distribution of the former austenite grain growth for the different heat treatment variants shown in Figure 4.

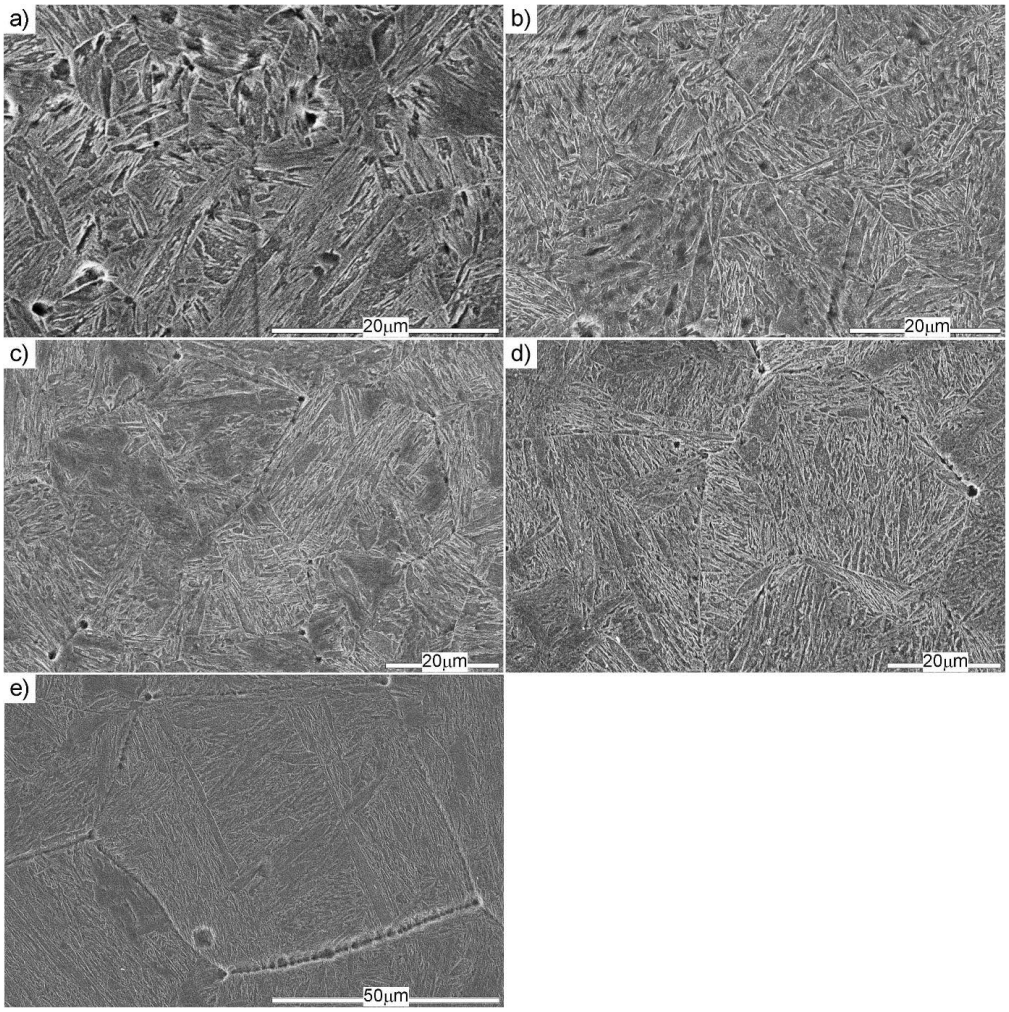

Figure 8. Micrographs showing martensitic packets in the Hardox 450 steel in the as-received state and under different annealing conditions: (**a**) in the as-received state; (**b**) 900 °C, 20 min; (**c**) 1000 °C, 20 min; (**d**) 1100 °C, 20 min; (**e**) 1200 °C, 20 min. Etched state, SEM.

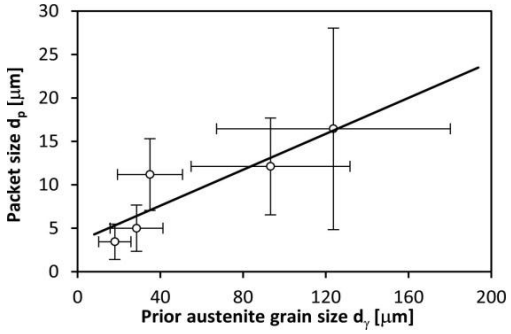

Figure 9. Relationship between the packet size and the prior austenite grain size in the Hardox 450 steel.

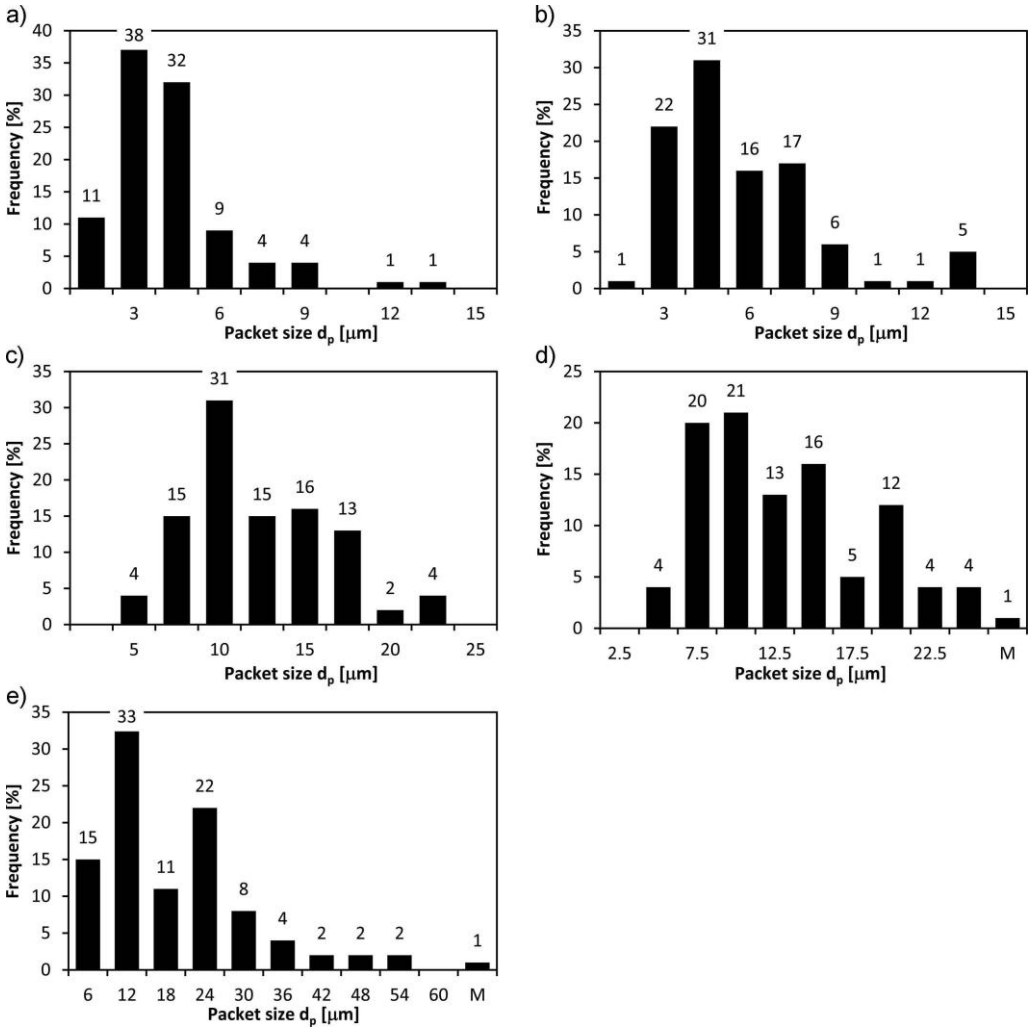

Figure 10. Distribution of martensite packet size in Hardox 450 steel with the prior austenite grain sizes: (**a**) 18 μm; (**b**) 28.5 μm; (**c**) 35 μm; (**d**) 93.3 μm, M—packet size more than 25 μm; (**e**) 123.7 μm, M—packet size more than 60 μm.

3.4. Fracture Analysis

Another way to determine the temperature of ductile-to-brittle transition is by direct analysis of the nature of the fracture. It is assumed that the criterion of impact strength (35 J/cm^2) corresponds to the occurrence of the mid-brittle and mid-ductile fracture [17].

Figure 11 summarizes the macroscopic views of fractures of the tested steel at temperature—40 °C in the as-received state and after different austenitizing temperatures. Figures 12–16 show representative SEM images of the fracture surfaces of the investigated steels.

Macroscopic analysis of the tested samples showed a significant divergence in the assessment of the embrittlement threshold based on the value of impact strength and direct analysis of the fracture. In all samples, there is a large central zone with typical facets for brittle fracture. In the case of the tested steel in the as-received state and after austenitizing at 900 °C, the plastic zones under the mechanical notch and in lateral edges shared respectively 28% and 30% of the whole fracture. In the case of samples austenitized at 1000 °C, the central brittle zone occupied more than 77%. Samples austenitized at higher temperatures were constantly characterized by nearly 100% fraction of brittle fracture—84% (for the sample austenitized at 1100 °C) and 89% (for the sample austenitized at 1200 °C). The fraction area of brittle fracture significantly increases by about 27% with increase in the austenitizing temperature.

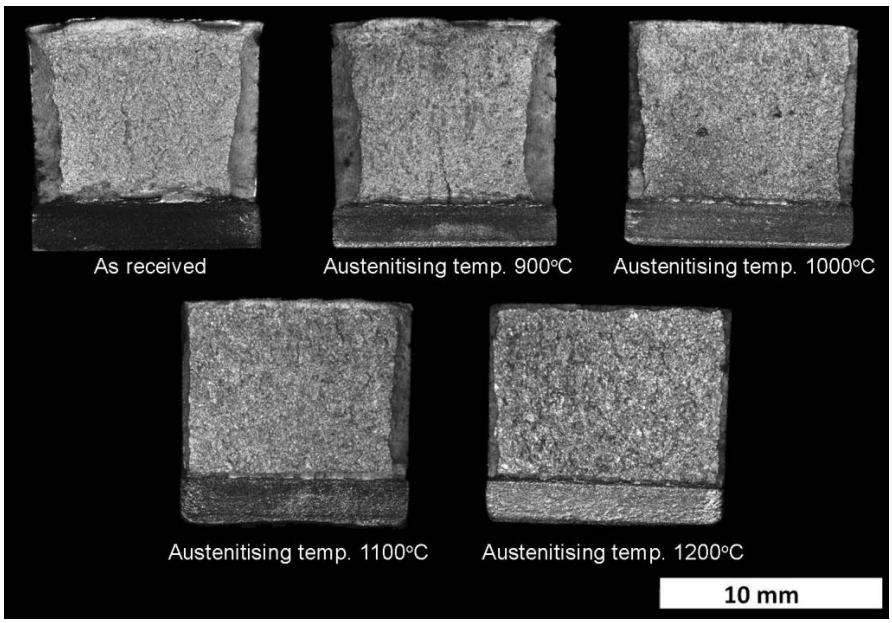

Figure 11. Macroscopic view of the fractures that occurred after the Charpy impact strength test of the as-received state sample and the samples austenitized at different temperatures.

Analysis of the fractures in the individual samples austenitized at different temperatures showed some differences in structure. The change in fracture morphology as a function of austenitization temperature (growth of the austenite grain) may be characterized based on the morphology and the fraction of cleavage ridges appearing in the analyzed fractures. With an increase in the austenitizing temperature, the fraction of plastic areas inside the grains decreases, and typically cleavable areas even appear, after which the fraction of the main cleavage ridges increases.

The fracture in the as-received sample is shown in Figure 12a–d. The lateral zones, as well as that under the mechanical notch, constitute the ductile fracture with voids of various diameters (Figure 12a,d). The plastic zone under the mechanical notch of the pitting structure is shown in the figure. The fracture partly shows the "flaky" structure. It is considered that such a fracture is created as a result of the slides and the subsequent decohesion and appearance of microcracks in the {100} planes. The connection of microcracks through shear of the walls dividing them gives the characteristic appearance of the fracture in the form of overlapping flakes. As a result, the fracture is initiated with plastic deformation—a slide—but the cracking itself runs in principle along the specific crystallographic planes [5]. The pits are parabolic in shape, which proves the action of tangent forces in the process of fracture formation. Additionally, smooth areas can be distinguished, free of typical pitting relief. The central zone is occupied by a so-called quasi-cleavage fracture (Figure 12b). This is typical of steels with a martensitic structure, as well as a bainitic one, at temperatures below the brittle fracture transition temperature. This type of fracture forms through cleavage cracking in small local areas, after which their combination into one cracking surface takes place as a result of the plastic deformation. Despite the fact that the facets here are similar to the cleavable ones due to the presence of the carved "river patterns," identification of the crystallographic planes is almost impossible. This is not a typical quasi-cleavage fracture because the system of "river patterns", while meandering, creates pits at the large surface whose structure can resemble a ductile fracture. The ridges of the quasi-cleavable facets are characterized by extensive topography, which also indicates large plastic deformation during their formation. Moreover, numerous transverse cracks were observed. In the plastic zones of the pitted structure, inclusion precipitations are stuck.

Figure 12c shows the fault, which extends above the crack surface, having marked at the shoulder the ductile fracture of the pitted structure, which could also be evidence that the small column from the

matrix was pulled (Figure 12c). One gets the impression that the columns joined the surfaces separated by cracking. If that was so, then we can speak of local breaking of the crack development. Thus, these photographs are proof of the very uneven and developed microrelief of the crack surfaces.

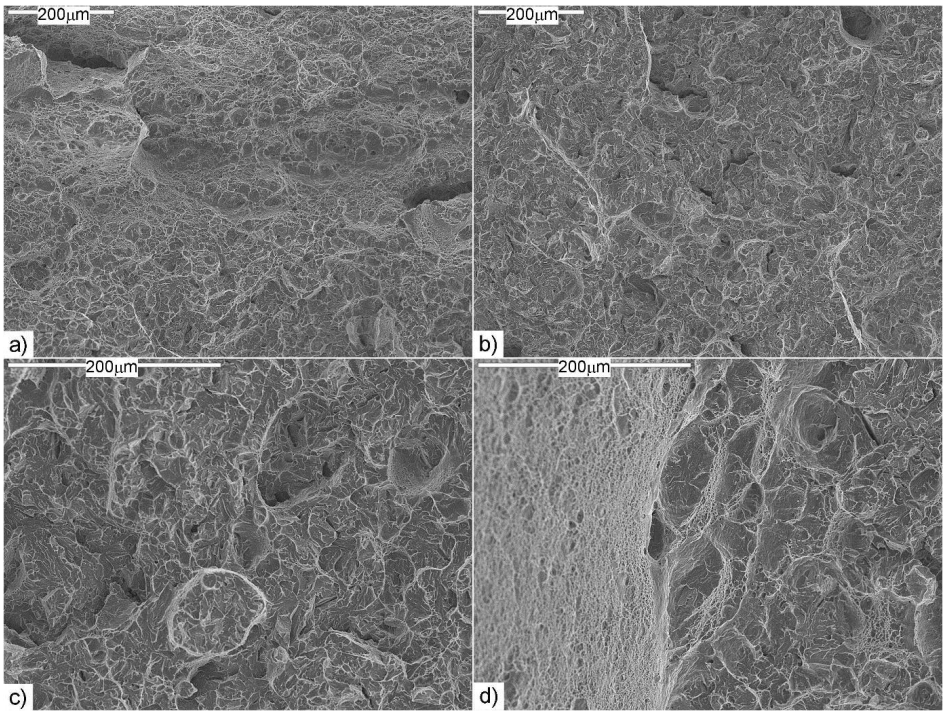

Figure 12. Fracture of the tested sample in the as-received state: (**a**) the zone under the mechanical notch; (**b**) the quasi-brittle central zone with visible ductile area; (**c**) the central zone with visible "small column"; (**d**) transition between the plastic lateral zone and the quasi-cleavage zone, SEM.

The fracture of the sample austenitized at a temperature of 900 °C is characterized by extensive topography; however, it does not differ in terms of quality from the fracture in the as-received state, although the value of the impact resistance varies greatly (Figure 13a–d). The characteristic feature is the appearance of a larger number of fine transverse cracks (Figure 13d). Under the mechanical notch, where the ductile fracture appears, the topography is very extensive (Figure 13a), and there is a large fracture of ductile fracture in the lateral zones, as well as in the central part of the sample, in the form of bands (Figure 13b). In the central part of the fracture, a large fracture of plastic zones appears with the characteristic pitted structure, which extends over the facets. The "river patterns" themselves combine into basins, with the characteristic plastic structure. Additionally, small columns were noticed, the lateral zones of which are built of the ductile fracture (Figure 13c). The central zone constitutes the quasi-cleavable fracture.

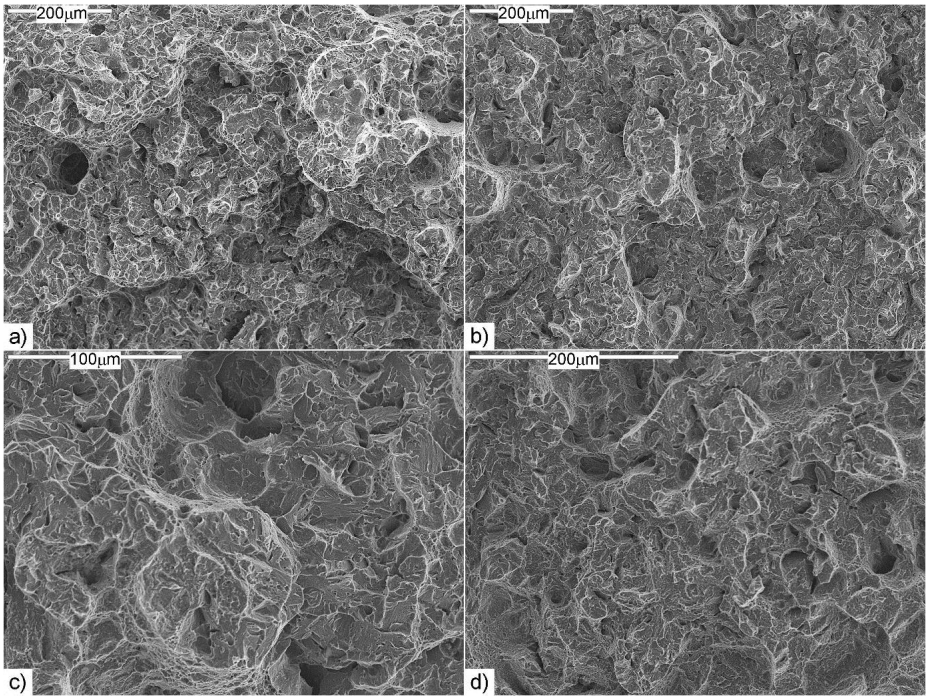

Figure 13. Fracture of the tested sample austenitized at 900 °C: (**a**) the zone under the mechanical notch; (**b**) the quasi-brittle central zone with visible ductile area; (**c**) the central zone with visible "small column"; (**d**) the quasi-cleavable zone with visible transverse cracks, SEM.

After austenitizing at a temperature of 1000 °C, despite a drop in the impact resistance value, the character of the fractures also changes insignificantly (Figure 14a–c). The topography is still extensive; in the central zone, the strained facets can be distinguished with characteristics of the "river patterns" relief. However, the cleavage ridges, where the typical ductile fracture appears, are narrower than in the case of the sample austenitized at a temperature of 900 °C (Figure 14a,b). Additionally, the characteristic small columns are visible (Figure 14c). Because of the characteristic "river patterns" relief, the surface of the fracture more closely resembles the quasi-cleavable fracture. The basins cross the whole grain. The appearance of these discontinuities means that the cracking ran not in a single crystallographic plane, but leapt from one plane to the other through shearing or the secondary cracking of the walls dividing them. It has been shown that this effect appears when the cracking front encounters screw dislocation, where the fault height is conditioned by the size of the Burgers vector [5]. The increase in energy absorbed during cracking is associated with the formation of the leaps, which is equivalent to a reduction of brittleness. The presence of the faults influences a change in direction of the cracking propagation. As a result, the growth of the crack is delayed in some sections, which entails a bending of its front, and this affects the merging of the adjacent faults, and their combination into the system of "river patterns".

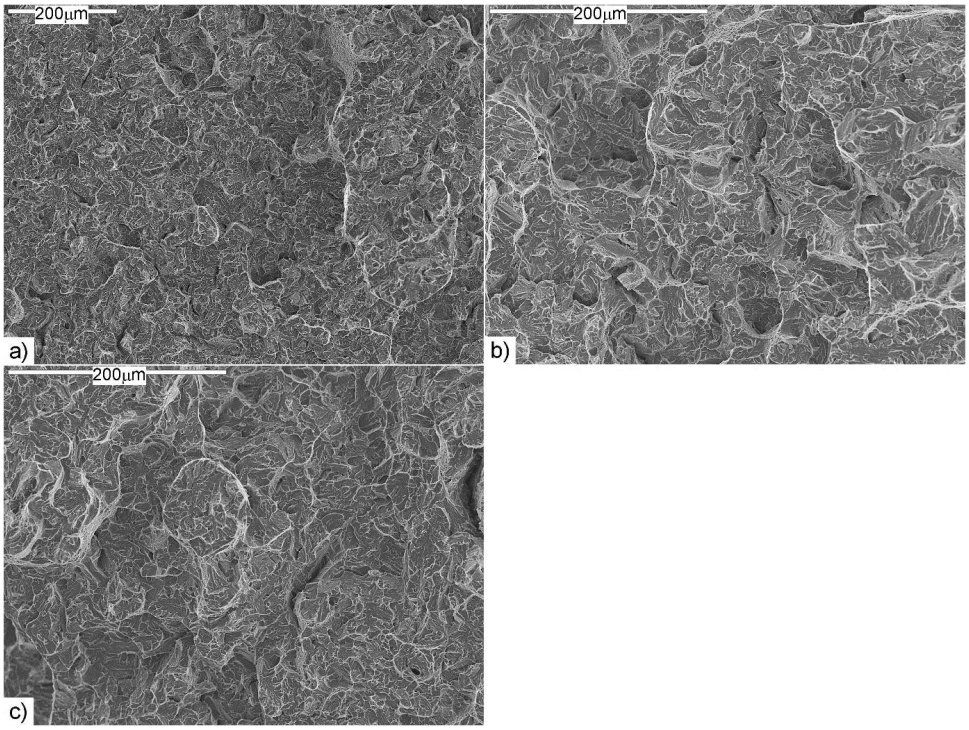

Figure 14. Fracture of the tested sample austenitized at 1000 °C: (**a**) the quasi-brittle central zone with visible ductile area; (**b**) the magnified central zone of the characteristic relief of "river patterns" with visible plastic ridges; (**c**) the central zone with visible "small column", SEM.

The appearance of abnormal grains and the increase in grain size as a result of austenitizing at a temperature of 1100 °C caused a drop in impact resistance below the criterion of 35 J/cm^2. This was reflected in minor qualitative changes of the character of the central zone of the fracture in comparison to the samples austenitized at lower temperatures (Figure 15a–c). It seems that the drop in impact resistance was influenced more by the smaller fracture of plastic zones under the mechanical notch and near the edges than by the fraction of these zones in the central part of the fracture. The plastic zone near the edge of the sample shows the "flaky" structure (Figure 15d). The surface of the fracture is characterized by extensive topography with larger hills and holes, and numerous transverse cracks were noticed. A large fraction of typically cleavable areas with the cleavage faults inside the grains was noticed (Figure 15b). The appearance of these areas caused a significant drop in the impact resistance value as compared to the samples austenitized at higher temperatures. The cracks continue to form the branching, but not as intensively as in the case of samples austenitized at lower temperatures, which could have been influenced by the increase in grain size of the tested steel. It is understood that the secondary slots propagate in the direct vicinity of the main slot, until they show the characteristic discontinuity (the slot is created by the whole system of small micro slots). One of the reasons for the formation of such micro slots is the appearance of micro faults in the fracture surface, which can be attributed to defects in the internal structure. In the case of crystalline bodies, such defects will be dislocations and the grain boundaries [5]. As shown in [3], the density of dislocations is higher in the case of steel with a finer grain.

After austenitizing at the highest temperature, the fraction of plastic zones is small; instead, in the central zone, we still have to deal with the quasi-cleavage fracture (Figure 16a,b). The facets created in this way are small and do not have clear boundaries. Moreover, the characteristic feature of quasi-cleavage is that the secondary cleavage faults are transformed into cleavage ridges of the surrounding facet. Pits can also be noticed, as characteristic features of ductile fracture (Figure 16b). The facets of the characteristic relief of "river patterns" combine through the so-called cleavage ridges

with features characteristic of ductile cracking as a result of plastic deformation. Mainly, they are located at lateral surfaces of the faults. Besides the quasi-cleavable areas, a significant fraction of typically cleavable areas was noticed (Figure 16a). The fracture topography is still extensive, and the transverse cracks and "small columns" appear; however, the holes and hills in the central zone are larger than in the case of fractures in samples austenitized at lower temperatures, which could be influenced by the coarse grain structure.

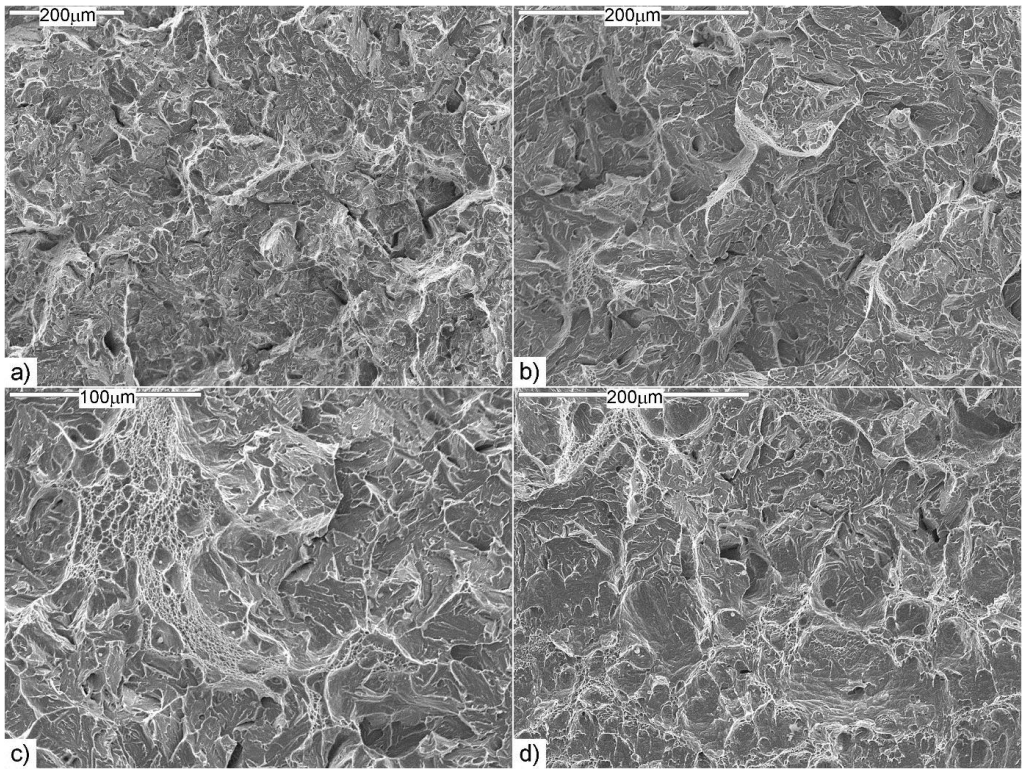

Figure 15. Fracture of the tested sample austenitized at 1100 °C: (**a**) the quasi-brittle central zone with visible ductile area; (**b**) the central zone with visible "small column" and cleavable zones; (**c**) the ductile band in the central zone; (**d**) plastic zone in the lower part of the sample (opposite to the mechanical notch), SEM.

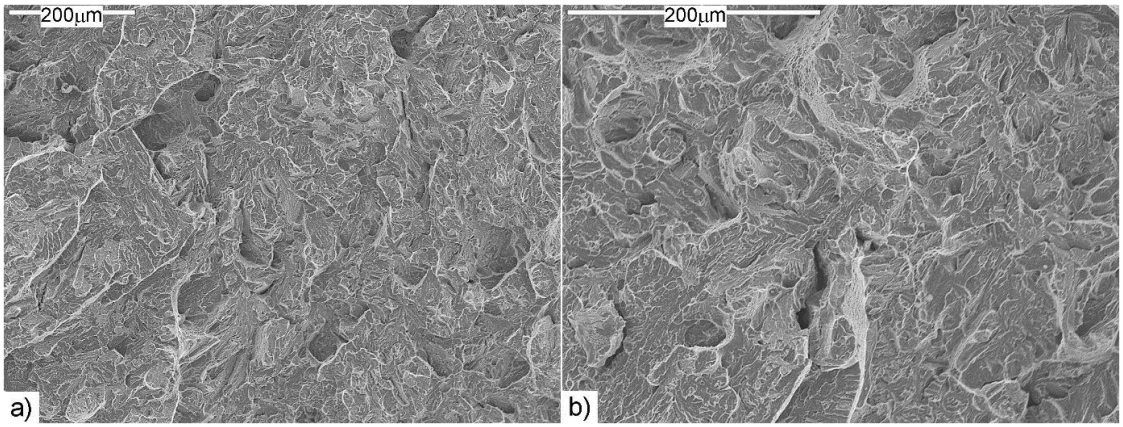

Figure 16. Fracture of the tested sample austenitized at 1200 °C: (**a**) the central zone of the fracture, visible small plastic areas and the typically cleavable areas; (**b**) the ductile bands and transverse crack in the central fracture zone, SEM.

4. Discussion

Selected mechanical properties for the analyzed steel in the as-received state and dependent on the austenitizing temperature have thus been shown, which has practical value. In this section, the values are to be dependent on the size of the austenite grains and packets of martensite. Figures 17 and 18 show the selected mechanical properties dependent on the size of the austenite grain in the analyzed steel and of the martensite packets. It can be noticed that, in the case of the impact resistance, the values were approximated with the exponential function with a good coefficient of correlation, while, in the case of the yield strength, the best correlation coefficient was obtained while approximating with the linear function.

Based on the achieved results, it can be stated that the plastic and not the strength properties are significantly more sensitive to a change in austenite grain size (especially when grain growth begins at lower austenitizing temperatures, even before the abnormal grains appear). In particular, the resistance of the tested steel to loads of dynamic character largely degrades, although the critical value of 35 J/cm^2 was not reached until the grains grew to about 90 μm. It can be concluded that the first phase of austenite grain growth is very critical in the process of reducing the mechanical properties.

In turn, the analysis of the impact of the martensite packet sizes on the yield strength has shown that, in the case of the lath martensite structure, the dependence described by the Hall-Petch relationship closely relates to the packet sizes as well as the effective martensite grain size in the low- and medium-carbon steel. It can be concluded that a change in the yield strength in the Hardox 450 steel corresponds with the inversion of the square root of the former austenite grain and the martensite packet size (Figure 17). However, it has to be underlined that the noted drop in the yield strength, as a result of the increase in grain size of the prior austenite from 18 μm to 124 μm (almost 700%), amounted only to 119 MPa (about 11%). In relation to the martensite, lowering the yield strength by the given value corresponded to an increase in the packet size of about 480% (3–16 μm). However, the impact of the increase in grain size of the former austenite and the packet size on the static tensile strength was not observed to be large.

Figure 18 presents the dependence between the grain size of the former austenite and martensite packets and the impact resistance value of the Hardox 450 steel. As a result of the increase in grain size of the former austenite from 18 μm to 124 μm, as well as the size of the packets, a more than 3.5-fold reduction in the impact resistance of the tested steel was noticed. This indicates a major influence of the packet size characteristic of martensitic steels on fracture work, especially at lower temperatures.

Undoubtedly, a change in the austenite grain size has an influence on impact resistance; thus, the martensite packets contributed to a decrease in the fraction of plastic zones near the fracture edge, as well as a change in character of the central quasi-cleavable zone, where a decrease in the fraction of the plastic ridges of cleavage occurred, the typical brittle facets appeared, and the means of propagation of the secondary cracks changed.

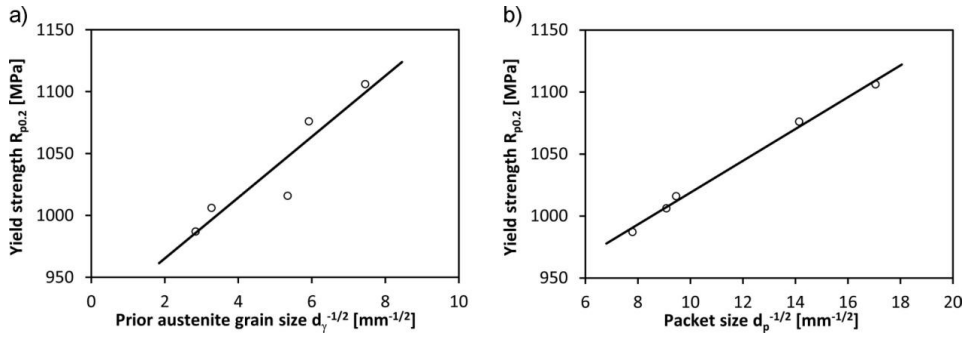

Figure 17. Dependence of the yield strength on the prior austenite grain size (**a**) and the martensite packet size (**b**) for the Hardox 450 steel.

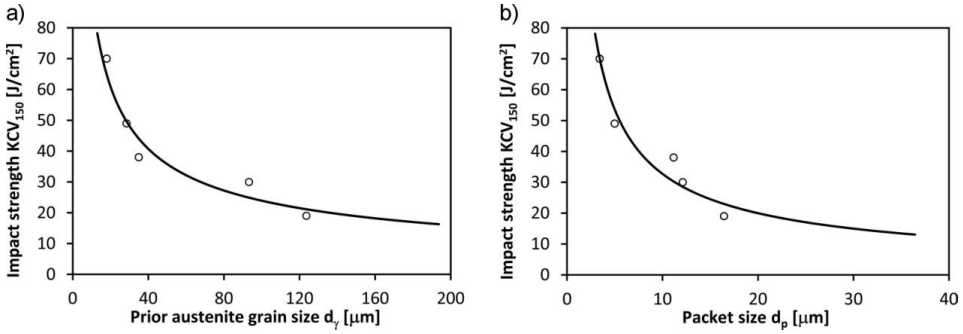

Figure 18. Influence of the prior austenite grain size (**a**) and martensite packet size (**b**) on the impact strength KCV_{150} at 233K (−40 °C) for the Hardox 450 steel.

In the Hardox 450 steel (independent of the applied variant of heat treatment), the value of the yield strength value is related to the classic Hall-Petch rule. In the case of martensitic structures, the effective size of the grains considered in the above rule constitutes the martensite laths arranged in the form of packets of identical crystallographic orientation. However, it has to be mentioned that the size of the martensite packets, being closely related to the size of the prior austenite grains, is not taken into account in the Hall-Petch rule as the factor determining the plastic properties of steels. Again, it has to be noted that, in the case of Hardox 450 steel, the main decisive factor on the plastic properties is the value of Charpy impact energy, the value of which (in contrast to percentage elongation A and the percentage reduction of area Z) decreased as a function of the state of heat treatment, despite maintaining high-strength parameters. It has to be stressed, however, that, for the analyzed group of steels, the plastic properties, in most cases, are analyzed on the basis of the fracture morphology obtained.

The greater impact of the grain size on the impact resistance than on strength properties can be explained by the greater sensitivity of the impact resistance not so much on the austenite grain size as on the size of the martensite packets. Similar conclusions were reached by the authors of [18,19], who developed the heat treatment of steel, enabling a reduction in austenite grain size that would result in high resistance combined with high ductility in minus temperatures. According to the author of [4], "grain refinement is accomplished by controlling the martensitic transformation to break up the crystallographic alignment between adjacent martensite laths, interrupting the cleavage fracture path. In this case, grain refinement does not ordinarily cause a substantial increase in strength, probably because {110} planes lie along the long axis of the laths, which are not significantly refined."

In summary, this study forms part of the current research on modern steel groups with higher resistance to abrasive wear. The growth of austenite grains is an important factor in the analysis of the microstructure, as the grain size has an effect on the kinetics of phase transformation. The microstructure, however, is closely related to the mechanical properties of the material such as yield strength, tensile strength, percentage elongation, and impact strength, as well as the morphology of the fractures that occur. Therefore, it is important to control the grain size of metals and metal alloys during processes connected with thermal treatment such as welding or cutting.

5. Conclusions

1. The steel analyzed in the as-received state is characterized by high-strength properties combined with high impact resistance at lower temperatures and by ductility.
2. The lowest average size of prior austenite grains noted for the as-received state was 18.0 ± 7.8 μm. Increasing the austenitizing temperature causes an increase in the average grain size, which, at 1200 °C, is 123.7 ± 56.5 μm. These changes can be approximated by a quadratic function.
3. The austenite grain size has a strong influence on the mechanical properties of the investigated steel. However, in comparison to the significant changes in impact resistance, the austenite grain

growth is accompanied by a small change in strength properties, i.e., the tensile strength and the yield strength.

4. As a result of increasing the grain size of the prior austenite from 18 μm to 124 μm, as well as the packet sizes, a more than 3.5-fold drop in the impact resistance of the tested steel was found. This indicates a major influence of the packet size characteristic of martensitic steels on the value of the fracture work, especially at lower temperatures.
5. Assuming the criterion of minimum impact strength is equal to 35 J/cm^2, this steel meets this criterion until the austenitization temperature reaches 1000 °C. However, after austenitizing at a temperature of 1100 °C, the impact strength of this steel was 30 J/cm^2, which is not much lower than the criterion cited.
6. The analysis of the influence of the martensite packets size on the yield strength showed that, in the case of the lath martensite structure, the dependence described by the Hall-Petch relation is closely related to packet size as well as the effective size of martensite grain in the low- and medium-carbon steel. It can be concluded that a change in the yield strength value of the Hardox 450 steel corresponds with the inverse of the square root from the grain size of the prior austenite and the packet size of the martensite.
7. Undoubtedly, the change in the size of the austenite grains and the martensite packets has an influence on the impact resistance, which contributed to a decrease in the fraction of plastic zones near the fracture edge and a change in the character of the central zone of the quasi-cleavable zone, where a decrease in the share of plastic cleavage ridges appeared, typical brittle facets appeared, and the means of propagation of the secondary cracks changed.

Author Contributions: Beata Białobrzeska contributed reagents/materials/analysis tools, conceived and designed the experiments, performed experiments, analysed data, wrote the paper; Łukasz Konat contributed reagents/materials/analysis tools, analysed data; Robert Jasiński conceived and designed the experiments performed experiments, analysed data.

Conflicts of Interest: The authors declare no conflict of interest.

References

1. Morito, S.; Tanaka, H.; Konishi, R.; Furuhara, T.; Maki, T. The morphology and crystallography of lath martensite in Fe-C alloys. *Acta Mater.* **2003**, *51*, 5323–5331. [CrossRef]
2. Wang, C.; Wang, M.; Shi, J.; Hui, W.; Dong, H. Effect of Microstructure Refinement on the Strength and Toughness of low alloy martenitic steel. *J. Mater. Sci. Technol.* **2007**, *23*, 659–664.
3. Prawoto, Y.; Jasmawati, N.; Sumeru, K. Effect of Prior Austenite Grain Size on the Morphology and Mechanical Properties of Martensite in Medium Carbon Steel. *J. Mater. Sci. Technol.* **2012**, *28*, 461–466. [CrossRef]
4. Morris, J.W., Jr. The Influence of Grain Size on the Mechanical Properties of Steel. In Proceedings of the International Symposium on Ultrafine Grained Steels, Fukuoka, Japan, 20–22 September 2001; Takaki, S., Maki, T., Eds.; Iron and Steel Institute of Japan: Tokyo, Japan, 2001; pp. 34–41.
5. Maciejny, A. *Kruchość Metali*; Wydawnictwo "Śląsk" Katowice: Katowice, Poland, 1973.
6. Esmailian, M. The effect of cooling rate and austenite grain size on the austenite to ferrite transformation temperature and different ferrite morphologies in microalloyed steels. *Iranian J. Mater. Sci. Eng.* **2010**, *7*, 7–14.
7. Lee, S.-J.; Lee, Y.-K. Prediction of austenite grain growth during austenitization of low alloy steels. *Mater. Des.* **2008**, *29*, 1840–1844. [CrossRef]
8. Dobrzański, L.A. *Podstawy Nauki o Materiałach i Metaloznawstwo*; WNT: Warsaw, Poland, 2003.
9. Krauss, G. *Steels, Processing, Structure, and Performance*; ASM International: Novelty, OH, USA, 2005.
10. Guimaraes, J.R.C.; Rios, P.R. Quantitative Interpretation of Martensite Microstructure. *Mater. Res.* **2011**, *14*, 97–101. [CrossRef]
11. Kitahara, H.; Ueji, R.; Tsuji, N.; Minamino, Y. Crystallographic features of lath martensite in low-carbon steel. *Acta Mater.* **2006**, *54*, 1279–1288. [CrossRef]

12. Manufacturer's Data. Available online: http://www.ssab.com/Global/HARDOX/Datasheets/en/168_HARDOX_450_UK_Data%20Sheet.pdf (accessed on 2 March 2015).
13. Dudziński, W.; Konat, Ł.; Pękalski, G. Structural and strength characteristics of wear-resistant martensitic steels. *Arch. Foundry Eng.* **2008**, *8*, 21–26.
14. Dudziński, W.; Konat, Ł.; Pękalska, L.; Pękalski, G. Structures and properties of Hardox 400 and Hardox 500 steels. *Inżynieria Materiałowa* **2006**, *3*, 139–142.
15. Konat, Ł. The Structure and Properties of Steel Hardox and Their Potential Application in the Conditions of Abrasive Wear and Dynamic Loads. Ph.D. Thesis, Wrocław University of Technology, Wrocław, Poland, 2007.
16. Gutérrez, N.Z.; Luppo, M.I.; Danon, C.A.; Caraballo, I.T.; Capdevila, C.; de Andrés, C.G. Heterogeneous austenite grain growth in martensitic 9Cr steel. Coupled influence of the initial metallurgical state and the heating rate. *Mater. Sci. Technol.* **2013**, *29*, 1254–1266. [CrossRef]
17. Wyrzykowski, J.W.; Pleszakow, E.; Sieniawski, J. *Odkształcenie i Pękanie Metali*; WNT: Warszawa, Poland, 1999.
18. Kim, H.J.; Kim, Y.H.; Morris, J.W., Jr. Thermal Mechanisms of Grain and Packet Refinement in a Lath Martensitic Steel. *ISIJ Int.* **1998**, *38*, 1277–1285. [CrossRef]
19. Morris, J.W., Jr.; Guo, Z.; Krenn, C.R. *Heat Treating: Steel Heat Treating in the New Millennium*; Midea, S.J., Pfaffmann, G.D., Eds.; ASM: Metals Park, OH, USA, 2000.